LETTER

doi:10.1038/nature10648

Dopamine neurons derived from human ES cells efficiently engraft in animal models of Parkinson's disease

Sonja Kriks[1,2]*, Jae-Won Shim[1,2]*, Jinghua Piao[1,3], Yosif M. Ganat[1,2], Dustin R. Wakeman[4], Zhong Xie[5], Luis Carrillo-Reid[5], Gordon Auyeung[1,3], Chris Antonacci[1,3], Amanda Buch[1,3], Lichuan Yang[6], M. Flint Beal[6], D. James Surmeier[5], Jeffrey H. Kordower[4], Viviane Tabar[1,3] & Lorenz Studer[1,2,3]

Human pluripotent stem cells (PSCs) are a promising source of cells for applications in regenerative medicine. Directed differentiation of PSCs into specialized cells such as spinal motoneurons[1] or midbrain dopamine (DA) neurons[2] has been achieved. However, the effective use of PSCs for cell therapy has lagged behind. Whereas mouse PSC-derived DA neurons have shown efficacy in models of Parkinson's disease[3,4], DA neurons from human PSCs generally show poor *in vivo* performance[5]. There are also considerable safety concerns for PSCs related to their potential for teratoma formation or neural overgrowth[6,7]. Here we present a novel floor-plate-based strategy for the derivation of human DA neurons that efficiently engraft *in vivo*, suggesting that past failures were due to incomplete specification rather than a specific vulnerability of the cells. Midbrain floor-plate precursors are derived from PSCs 11 days after exposure to small molecule activators of sonic hedgehog (SHH) and canonical WNT signalling. Engraftable midbrain DA neurons are obtained by day 25 and can be maintained *in vitro* for several months. Extensive molecular profiling, biochemical and electrophysiological data define developmental progression and confirm identity of PSC-derived midbrain DA neurons. *In vivo* survival and function is demonstrated in Parkinson's disease models using three host species. Long-term engraftment in 6-hydroxy-dopamine-lesioned mice and rats demonstrates robust survival of midbrain DA neurons derived from human embryonic stem (ES) cells, complete restoration of amphetamine-induced rotation behaviour and improvements in tests of forelimb use and akinesia. Finally, scalability is demonstrated by transplantation into parkinsonian monkeys. Excellent DA neuron survival, function and lack of neural overgrowth in the three animal models indicate promise for the development of cell-based therapies in Parkinson's disease.

Recent mouse genetic studies have demonstrated an important role for the transcription factor *FOXA2* during midbrain DA neuron development[8,9]. A unique feature of the developing midbrain is the coexpression of the floor-plate (FP) marker FOXA2 and the roof plate marker LMX1A. Normally, FP and roof plate cells are located at distinct positions in the central nervous system (ventral versus dorsal) and show diametrically opposed patterning requirements[10,11]. We recently reported the derivation of FP precursors from ES cells[12] using a modified dual-SMAD inhibition protocol[13]. Canonical Wnt signalling is important for both roof plate function[14] and midbrain DA neuron development[15]. We therefore proposed that WNT activation may induce LMX1A expression and neurogenic conversion of PSC-derived midbrain FP towards DA neuron fate. Here we report that exposure to CHIR99021 (CHIR), a potent GSK3B inhibitor known to strongly activate WNT signalling[16], induces LMX1A in FOXA2+ FP precursors (Fig. 1a). CHIR was much more potent than recombinant WNT3A or WNT1 at inducing LMX1A expression (data not shown). The efficiency of LMX1A induction was dependent on the timing of CHIR exposure with a maximum effect from day 3 to day 11 (Supplementary Fig. 1). CHIR was the most critical factor for inducing coexpression of FOXA2/LMX1A, while other factors such as FGF8 had only marginal effects (Supplementary Fig. 2). Induction of FOXA2/LMX1A coexpression required strong activation of SHH signalling using purmorphamine, a small molecule agonist, alone or in combination with recombinant SHH (Supplementary Fig. 3). Treatment with SHH agonists (purmorphamine + SHH) and FGF8 (S/F8) in the absence of CHIR showed significantly lower expression of FOXA2 by day 11 and complete lack of LMX1A expression (Fig. 1a, b). Dual SMAD inhibition (exposure to LDN193189 + SB431542, 'LSB') did not yield FOXA2-expressing cells, but a subset of LMX1A+ cells (Fig. 1a, b). The anterior marker OTX2 was robustly induced in LSB- and LSB/S/F8/CHIR-treated cultures, but not under LSB/S/F8 conditions (Fig. 1a, c). Systematic comparisons of the three culture conditions (Fig. 1d) were performed using global temporal gene expression profiling. Hierarchical clustering of differentially expressed genes segregated the three treatment conditions by day 11 of differentiation (Supplementary Fig. 4a). *FOXA1*, *FOXA2* and several other SHH downstream targets including *PTCH1* were among the most differentially regulated transcripts in LSB/S/F8/CHIR versus LSB treatment sets (Fig. 1e). Expression of *LMX1A*, *NGN2* (also known as *NEUROG2*) and *DDC* indicated establishment of midbrain DA neuron precursor fate already by day 11 (Fig. 1e, f). In contrast, LSB cultures were enriched for dorsal forebrain precursor markers such as *HES5*, *PAX6*, *LHX2* and *EMX2*. Direct comparison of LSB/S/F8/CHIR versus LSB/S/F8 treatment (Fig. 1f) confirmed selective enrichment for midbrain DA precursor markers in LSB/S/F8/CHIR group and suggested hypothalamic precursor identity in LSB/S/F8-treated cultures based on the differential expression of *RAX*, *SIX3* and *SIX6* (ref. 17) (see also *POMC* and *OTP* expression in Fig. 2d below). The full list of differentially expressed transcripts (Supplementary Tables 1 and 2) and gene ontology analysis (Supplementary Fig. 4b) (DAVID; http://david.abcc.ncifcrf.gov, ref. 18) confirmed enrichment for canonical WNT signalling upon CHIR treatment (raw data available at the Gene Expression Omnibus). Comparative temporal gene expression analysis for markers of midbrain DA precursors (Fig. 1g) versus anterior and ventral non-DA fates (Fig. 1h) partitioned the three induction conditions into (1) LSB: dorsal forebrain; (2) LSB/S/F8: ventral/hypothalamic; (3) LSB/S/F8/CHIR: midbrain DA identity.

[1]Center for Stem Cell Biology, Memorial Sloan-Kettering Cancer Center, 1275 York Avenue, New York, New York 10065, USA. [2]Developmental Biology Program, Memorial Sloan-Kettering Cancer Center, 1275 York Avenue, New York, New York 10065, USA. [3]Department of Neurosurgery, Memorial Sloan-Kettering Cancer Center, 1275 York Avenue, New York, New York 10065, USA. [4]Department of Neurological Sciences, Rush University Medical Center, Chicago, Illinois 60612, USA. [5]Department of Physiology, Feinberg School of Medicine, Northwestern University, Chicago, Illinois 60611, USA. [6]Department of Neurology and Neuroscience, Weill Medical College of Cornell University, New York Presbyterian Hospital, 525 East 68th Street, New York, New York 10021, USA.
*These authors contributed equally to this work.

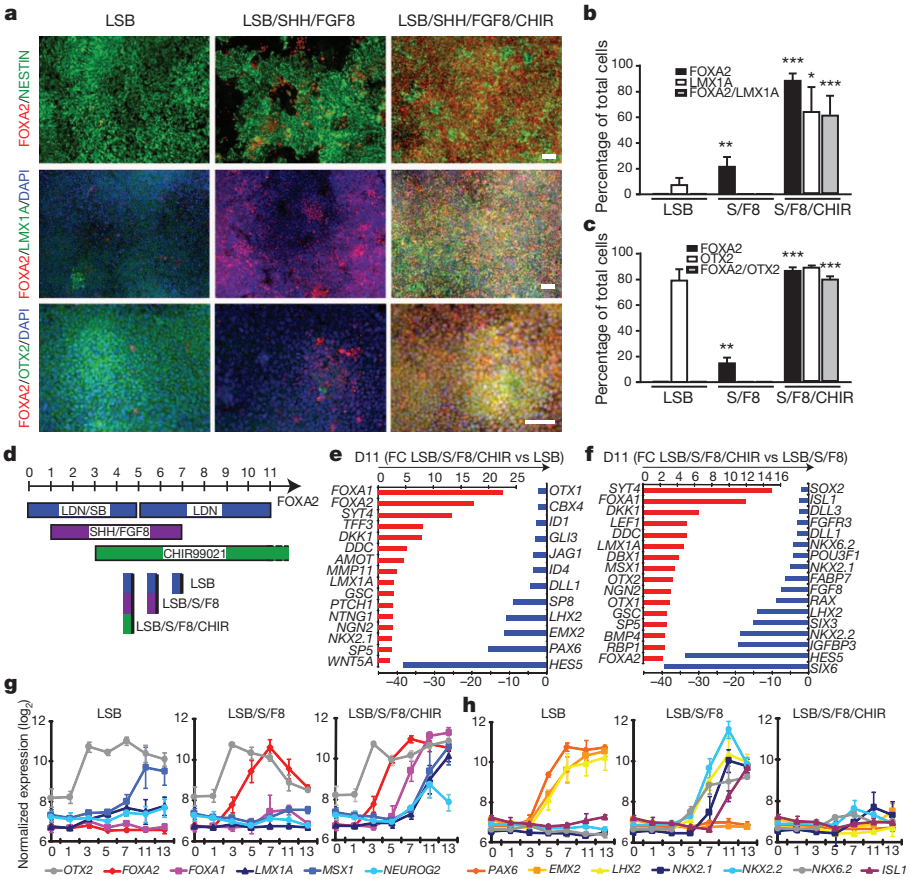

Figure 1 | Induction and neurogenic conversion of ES-cell-derived midbrain FP precursors is dependent on CHIR addition. **a**, Immunocytochemistry at day 11 for FOXA2 (red), NESTIN (green, upper panels), LMX1A (green, middle panels) and OTX2 (green, lower panels). **b**, **c**, Quantification of the data presented in **a**; mean ± s.e.m., $n = 3$ (independent experiments): $***P < 0.001$; $**P < 0.01$; $*P < 0.05$ (compared to LSB, Dunnett test). **d**, Diagram of culture conditions. **e**, **f**, Selected lists of differentially expressed transcripts at day 11 comparing LSB/S/F8/CHIR versus LSB (**e**) or versus LSB/S/F8 (**f**). **g**, **h**, Temporal gene expression analysis for markers of midbrain DA precursor (**g**), forebrain and ventral non-DA precursor identity (**h**). Scale bars, 50 μm.

By day 25, all three conditions yielded TUJ1+ neurons (Fig. 2a) and cells expressing TH, the rate-limiting enzyme in the synthesis of DA. However, only the LSB/S/F8/CHIR group yielded TH+ cells coexpressing LMX1A and FOXA2 as well as the nuclear receptor NURR1 (also known as NR4A2) (Fig. 2a, b). Comparing gene expression in day 13 versus day 25 cultures confirmed robust induction of postmitotic DA neuron markers (Fig. 2c). Characterizing DA neuron identity at day 25 in comparison to LSB and LSB/S/F8 showed enrichment for known

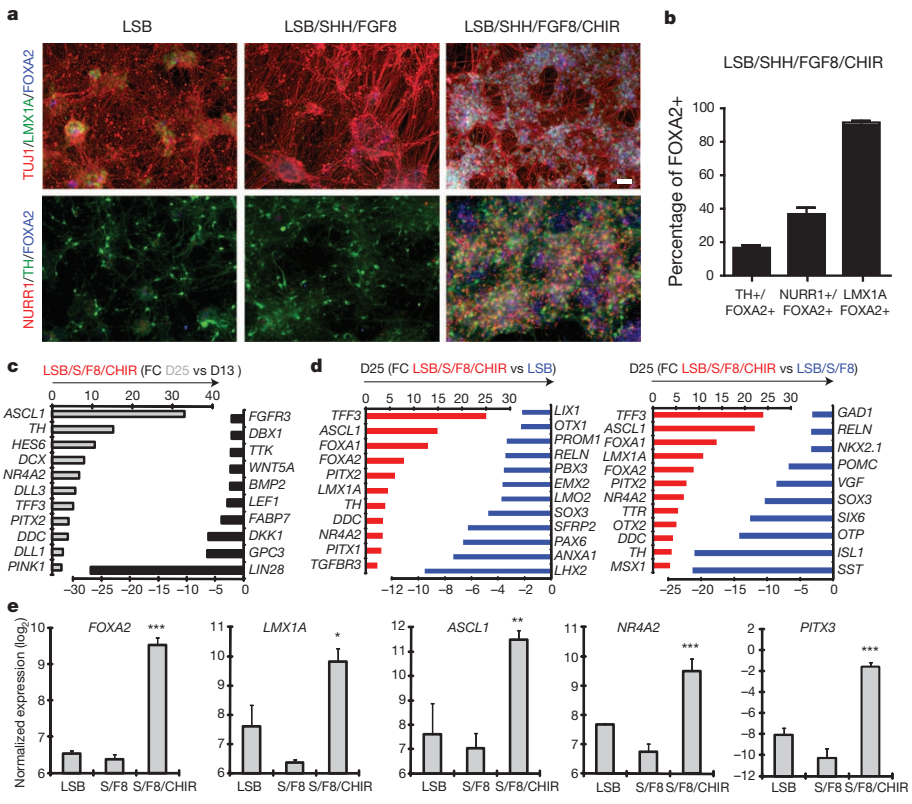

Figure 2 | Immunocytochemical and molecular analysis of midbrain DA neuron fate in LSB/S/F8/CHIR-treated versus LSB/S/F8 (hypothalamic) and forebrain LSB (dorsal forebrain) fates. **a**, Immunocytochemistry at day 25 for coexpression of FOXA2 (blue) with Tuj1(red)/LMX1A(green) (upper panels) and NURR1(red)/TH(green) (lower panels). **b**, Quantitative coexpression analysis for LSB/S/F8/CHIR; mean ± s.e.m., $n = 3$ (independent experiments). **c**, **d**, Global gene expression analysis at day 25 (quadruplicates each). Selected lists of differentially expressed transcripts comparing day 13 versus day 25 in LSB/S/F8/CHIR (**c**) LSB/S/F8/CHIR versus LSB (**d**, left panel) and LSB/S/F8 (**d**, right panel). **e**, Gene expression analysis for key midbrain DA neuron markers. Significance compared to LSB (Dunnett test): $***P < 0.001$; $**P < 0.01$; $*P < 0.05$. Scale bars, 50 μm.

midbrain DA neuron transcripts and identified multiple novel candidate markers (Fig. 2d, Supplementary Tables 3–5 and Supplementary Fig. 4b). For example, the transcript most highly enriched in LSB/S/F8/CHIR (midbrain DA group) was *TFF3*, a gene not previously associated with midbrain DA neuron development, but highly expressed in the human substantia nigra (Supplementary Fig. 4c; Allen Brain Atlas http://human.brain-map.org). Similar data were obtained for *EBF1*, *EBF3* (Supplementary Fig. 4c) as well as *TTR*, a known transcriptional target of FOXA2 in the liver[19]. We observed enrichment of several *PITX* genes, and *PITX3*, a classic marker of midbrain DA neurons, was also expressed robustly at day 25 of differentiation (Fig. 2e). Finally, both midbrain FP and DA neuron induction was readily reproduced in independent ES cell and human induced PSC lines (Supplementary Fig. 5). Our data demonstrate that the LSB/S/F8/CHIR protocol yields cells expressing a marker profile matching midbrain DA neuron fate.

We next proceeded to determine the *in vitro* and *in vivo* properties of FP-derived DA neurons in comparison to DA neurons obtained via a neural rosette intermediate[3] (Supplementary Fig. 6). Patterning of neural rosettes represents the currently most widely used strategy for deriving DA neurons from PSCs[2,6,20]. Both FP- and rosette-based protocols were efficient at generating TH+ neurons capable of long-term *in vitro* survival (day 50 of differentiation; Fig. 3a). However, the percentage of TH+ cells was significantly higher in FP-derived cultures (Fig. 3b). Whereas TH+ cells in both protocols showed co-expression of NURR1, only FP-derived DA neurons coexpressed FOXA2 and LMX1A (Fig. 3a,b). Few GABA- (γ-aminobutyric acid) and serotonin (5-HT)-positive neurons were observed (Fig. 3c). DA, and its metabolites DOPAC (3,4-dihydroxy-phenylacetic acid)and HVA (homovanillic acid), were present in cultures generated with either protocol, but DA levels were approximately eight times higher in FP cultures (Fig. 3d, e). Midbrain DA neurons showed extensive fibre outgrowth and robust expression of mature neuronal markers including synapsin, dopamine transporter (DAT) and G-protein-coupled, inwardly rectifying potassium channel (KCNJ6 (Kir3.2), also called GIRK2), expressed in substantia nigra pars compacta (SNPC) DA neurons (Fig. 3f and Supplementary Fig. 7).

SNPC DA neurons *in vivo* show an electrophysiological phenotype that differentiates them from most other neurons in the brain. In particular, they spike spontaneously at a slow (1–3 Hz) rate. Moreover, this slow spiking is accompanied by a slow, sub-threshold oscillatory potential[21,22]. After 2–3 weeks *in vitro*, these same physiological features are shown by SNPC DA neurons grown from early postnatal mice (data not shown). The DA neurons differentiated from ES cells consistently (4/4) had this distinctive physiological phenotype (Fig. 3g–i). Future studies will be required to determine whether all features of SNPC DA neurons are recapitulated by the ES cell DA neurons *in vitro* or whether full differentiation will require maturation *in vivo*. However, our data indicate that FP-derived DA neurons do show the cardinal physiological features of mature SNPC DA neurons.

A major challenge in the field has been the ability to generate PSC-derived midbrain DA neurons that functionally engraft *in vivo* without the risk of neural overgrowth[7] or inappropriate differentiation into non-midbrain neurons[23]. On the basis of fetal tissue transplantation studies[24] we proposed that the time of cell cycle exit, marked by expression of NURR1 (ref. 25), may be a suitable stage for grafting (~day 25 of differentiation, Fig. 2). Initial studies using day 25 cells in non-lesioned adult mice showed robust survival of PSC-derived FOXA2+/TH+ neurons at 6 weeks after transplantation (Supplementary Fig. 8). We next addressed whether FOXA2+/TH+ cells survive long-term in parkinsonian hosts without resulting in neural overgrowth. To this end, we made 6-hydroxy-dopamine (6-OHDA) lesions[3] in *NOD-SCID IL2Rgc* null mice, a strain that efficiently supports xenograft survival with particular sensitivity for exposing rare tumorigenic cells[26]. Both FP- and rosette-derived cultures were grafted (1.5×10^5 per animal) without prior purification to reveal potential

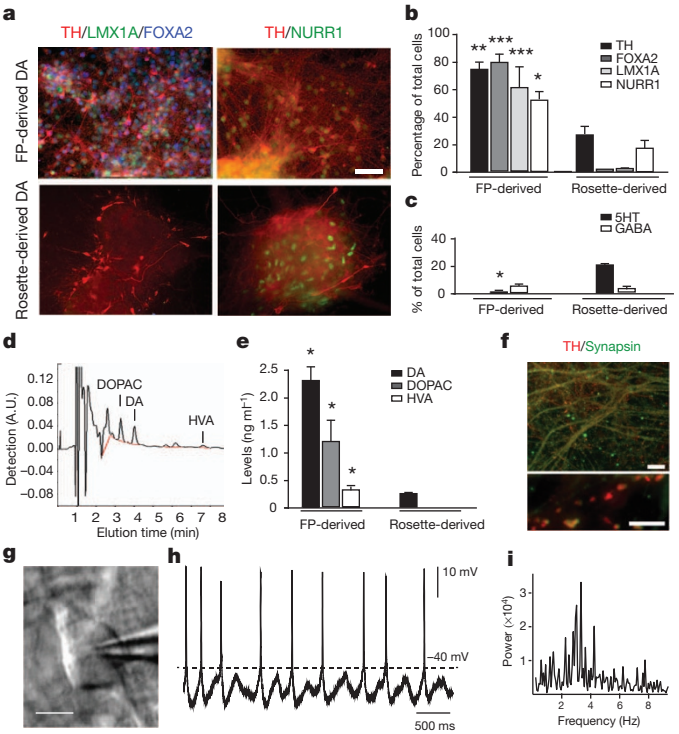

Figure 3 | *In vitro* maturation and functional characterization of FP versus rosette-derived midbrain DA neurons. **a**, Immunocytochemistry at day 50 for TH (red), with LMX1A (green) and FOXA2 (blue; left panels) and NURR1 (green, right panels). **b**, Quantification of TH+, FOXA2+, LMX1A+ and NURR1+ cells in rosette- versus FP-derived (LSB/S/F8/CHIR) cultures. **c**, Quantification of serotonin+ (5-HT), and GABA+ neuronal subtypes at day 50 in rosette- versus FP-derived cultures. **d**, **e**, HPLC analysis for DA and metabolites. **d**, Representative HPLC chromatogram in a sample of FP-derived cultures. A.U., arbitrary units. **e**, Levels of DA, DOPAC and HVA in FP- and rosette-derived cultures. **f**, Immunocytochemistry in FP-derived cultures (day 80) for TH (red) and synapsin (green). **g**–**i**, Electrophysiological analyses of FP cultures at day 80. Phase contrast image of a patched neuron (**g**) and corresponding recordings (**h**). **i**, Power analysis showing membrane potential oscillations characteristic of DA neuron identity (2~5 Hz). Mean ± s.e.m.; significance (panels **b**, **c**, **e**) comparing FP versus rosette-derived cultures (Student's *t*-test): ***$P < 0.001$; **$P < 0.01$; *$P < 0.05$. Scale bars: 50 μm in **a**, 20 μm in **f** upper panel and 5 μm in **f** lower panel, and 20 μm in **g**.

contaminating cells with proliferative potential. Four and a half months after transplantation FP-derived DA neuron grafts showed a well-defined graft core composed of TH+ cells coexpressing FOXA2 and human-specific NCAM (Fig. 4a–c). Functional analysis showed a complete rescue of amphetamine-induced rotation behaviour. In contrast, rosette-derived grafts had few TH+ neurons, did not produce significant reductions in rotation behaviour (Fig. 4d) and showed massive neural overgrowth (graft volume > 20 mm^3; Supplementary Fig. 9). Extensive overgrowth reported here as compared to previous work with rosette-derived DA grafts[27,28] is likely due to the longer survival periods (4.5 months versus 6 weeks), lack of fluorescence-activated cell sorting purification before transplantation and choice of *NOD-SCID IL2Rgc* null host. The number of proliferating Ki-67+ cells was minimal in FP-derived grafts (<1% of total cells), while rosette-derived grafts retained pockets of proliferating neural precursors. Neural overgrowth is thought to be caused by primitive anterior neuroectodermal cells within the graft[6,29]. This hypothesis was supported by the expression of the forebrain marker FOXG1 in rosette-derived but not FP-derived grafts. A small percentage of astroglial cells were present in both FP- and rosette-derived grafts, although most GFAP+ cells were negative for human markers, indicating host origin (Supplementary Fig. 9).

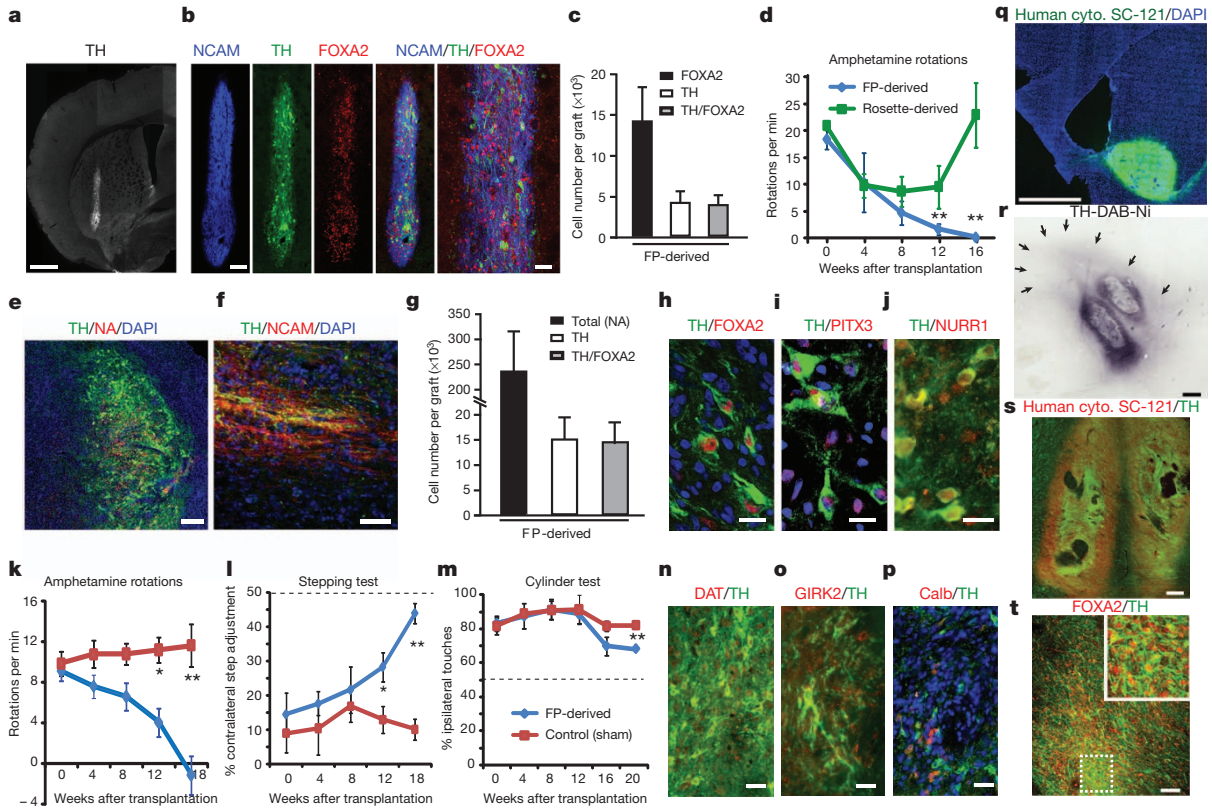

Figure 4 | *In vivo* survival and function of FP-derived human DA neurons in mouse, rat and monkey Parkinson's disease hosts. a–d, 6-OHDA-lesioned adult mice (*NOD-SCID IL2Rgc* null strain). **a**, TH expression and graft morphology at 4.5 months after transplantation. **b**, Expression of human-specific marker (NCAM, blue), TH (green) and FOXA2 (red). **c**, Quantification of FOXA2+ and TH+ cells in FP-derived grafts (mean ± s.e.m., $n = 4$ at 4.5 months after grafting). **d**, Amphetamine-induced rotation analysis in FP- (blue) versus rosette-derived (green) grafts. Scale bars: 500 μm in **a**, and 100 and 40 μm in **b** (left and right panels, respectively). **e–p**, 6-OHDA-lesioned adult rats. **e**, **f**, Immunohistochemistry for TH (green) and human-specific markers (red) human nuclear antigen NA (**e**) and NCAM (**f**). **g**, Stereological quantification of NA+, TH+ and TH+ cells co-expressing FOXA2 (average graft volume = 2.6 ± 0.6 mm^3). **h–j**, Coexpression of TH (green) with FOXA2 (**h**), PITX3 (**i**) and NURR1 (**j**) (all three red). **k–m**, Behavioural analysis in FP- versus sham-grafted animals. **k**, Amphetamine-induced rotational asymmetry. **l**, Stepping test: measuring forelimb akinesia in affected versus non-affected side. **m**, Cylinder test: measuring ipsi- versus contra-lateral paw preference. Grafted animals showed significant improvement in all three tests ($P < 0.01$ at 4.5–5 month; $n = 4$–6 each). **n–p**, Immunohistochemistry for TH (green) and coexpression (red) with DAT (**n**), GIRK2 (**o**) and calbindin (**p**). Significance levels (panels **d**, **k**, **l**, **m**): $^{**}P < 0.01$; $^{*}P < 0.05$). Scale bars: 200 μm in **e**, 50 μm in **f**, 20 μm in **h–j** and 40 μm in **n–p**. **q–t**, Adult MPTP-lesioned rhesus monkeys. **q**, Representative graft at 1 month after transplantation expressing human specific cytoplasm (cyto.) marker SC-121 (green). **r**, TH expression in graft with surrounding TH+ fibres (arrows). **s**, Coexpression of SC-121 (red) and TH (green). **t**, Coexpression of FOXA2 (red) and TH+ (green). Scale bars: 2 mm for **q**, 500 μm for **r**, 200 μm for **s**, and 50 μm for **t**.

Our results in *NOD-SCID IL2Rgc* null mice demonstrated robust long-term survival of FOXA2+/TH+ neurons, complete reversal of amphetamine-induced rotation behaviour and lack of neural overgrowth. However, some of these outcomes could be attributable to the specific use of *NOD-SCID IL2Rgc* null mice. To test this hypothesis, FP-derived DA neuron cultures (2.5×10^5 cells) were transplanted in adult 6-OHDA-lesioned rats immunosuppressed pharmacologically using cyclosporine A. Five months after transplantation graft survival was robust (Fig. 4e–h) with an average of more than 15,000 TH+ cells coexpressing FOXA2 (Fig. 4g) and human nuclear antigen (Fig. 4e); TH+/NCAM+ fibres emanated from the graft core into the surrounding host striatum (Fig. 4f). In addition to FOXA2, TH+ cells expressed midbrain DA neuron markers PITX3 and NURR1 (Fig. 4h–j). Behavioural analyses showed complete rescue of amphetamine-induced rotational asymmetry in contrast to sham-grafted animals (Fig. 4k). Grafted animals also showed improvements in the stepping test (Fig. 4l) measuring forelimb akinesia and in the cylinder test (Fig. 4m), assays that do not depend on pharmacological stimulation of the DA system. The late onset of recovery (approximately 3–4 months after transplantation) is expected for human DA neurons and depends on the rate of *in vivo* maturation including levels of DAT expression (Fig. 4n). The presence of TH+ cells expressing Kir3.2 channels or calbindin indicate that both SNPC (A9) and ventral tegmental area (A10) DA neurons are present in the graft (Fig. 4o, p). As in mice (Supplementary Fig. 9), serotonergic and GABAergic cells were rare (<1% of total cells), as were the mostly host-derived GFAP+ glial cells (7% of total cells; Supplementary Fig. 10). While few serotonin+ neurons were detected in the graft, we observed human NCAM-negative, likely host-derived serotonergic fibres (Supplementary Fig. 10). Our results demonstrate excellent graft survival and behavioural outcome in two independent murine models. However, the number of DA neurons required in a mouse or rat brain represents only a fraction of the cells needed in a human. To test the scalability of our approach, we performed pilot grafting studies in two adult 1-methyl-4-phenyl-1,2,3,6-tetrahydropyridine (MPTP)-lesioned rhesus monkeys. We readily obtained batches of 5×10^7 transplantable DA neuron precursors by day 25 of differentiation using the FP-based protocol. Cells were injected at three locations (posterior caudate and pre-commissural putamen) on each side of the brain (six tracts in total, 1.25×10^6 cells per tract), and the animals were immunosuppressed with cyclosporine-A. One side of the brain was injected with DA precursors from a green fluorescent protein (GFP)-expressing subclone of H9, while the other side was engrafted with cells derived from unmarked H9 cells. One month after transplantation, we observed robust survival of midbrain DA neurons based on expression of GFP (Supplementary Fig. 11) and the human-specific cytoplasmic

marker (SC-121) (Fig. 4q). Each graft core was surrounded by a halo of TH+ fibres extending up to 3 mm into the host (Fig. 4r). The graft cores were composed of TH+ neurons coexpressing SC-121 (Fig. 4s) and FOXA2 (Fig. 4t). Areas within the graft contained Iba1+ host microglia (Supplementary Fig. 11), indicating incomplete immunosuppression.

In conclusion, we present a novel FP-based PSC differentiation protocol that faithfully recapitulates midbrain DA neuron development. Access to cells with the cardinal features of midbrain DA neurons will enable a broad range of biomedical applications such as basic developmental studies, high-throughput drug discovery and Parkinson's disease-iPSC based disease modelling. Importantly, our study establishes a means of obtaining a scalable source of FOXA2+/TH+ neurons for neural transplantation—a major step on the road towards considering a cell based therapy for Parkinson's disease.

METHODS SUMMARY

Human ES cell (H9, H1) and iPSC lines (2C6 and SeV6) were subjected to a modified dual SMAD-inhibition-based[13] FP induction[12] protocol. Exposure to SHH C25II, purmorphamine, FGF8 and CHIR were optimized for midbrain FP and DA neuron yield (see Fig. 1d). Following FP induction, further maturation was carried out in Neurobasal/B27 medium supplemented with ascorbic acid, BDNF, GDNF, TGFβ3 and dibutyryl (db) cyclic AMP (see full methods for details). The resulting DA neurons were subjected to extensive phenotypic characterization via immunocytochemistry, quantitative PCR with reverse transcription (qRT–PCR), gene expression profiling, high-performance liquid chromatography (HPLC) analysis for DA and *in vitro* electrophysiological recordings. *In vivo* studies were performed in 6-hydroxydopamine-lesioned, hemiparkinsonian rodents (adult *NOD-SCID IL2Rgc* mice and Sprague Dawley rats) as well as in two adult rhesus monkeys treated with carotid injections of MPTP. DA neurons were injected stereotactically in the striata of the animals (1.5×10^5 cells in mice, 2.5×10^5 cells in rats) and a total of 7.5×10^6 cells (distributed in six tracts; three on each side of brain) in monkeys. Behavioural assays were performed at monthly intervals after grafting, including amphetamine-mediated rotational analysis as well as a test for focal akinesia ('stepping test') and forelimb use (cylinder test). Rats and mice were killed at 18–20 weeks and the primates at 1 month after grafting. Characterization of the grafts was performed via stereological analyses of cell numbers and graft volumes and comprehensive immunohistochemistry.

Full Methods and any associated references are available in the online version of the paper at www.nature.com/nature.

Received 22 August; accepted 19 October 2011.

Published online 6 November 2011; corrected 21 December 2011 (see full-text HTML version for details).

1. Li, X. J. *et al.* Specification of motoneurons from human embryonic stem cells. *Nature Biotechnol.* **23,** 215–221 (2005).
2. Perrier, A. L. *et al.* From the cover: derivation of midbrain dopamine neurons from human embryonic stem cells. *Proc. Natl Acad. Sci. USA* **101,** 12543–12548 (2004).
3. Tabar, V. *et al.* Therapeutic cloning in individual parkinsonian mice. *Nature Med.* **14,** 379–381 (2008).
4. Wernig, M. *et al.* Neurons derived from reprogrammed fibroblasts functionally integrate into the fetal brain and improve symptoms of rats with Parkinson's disease. *Proc. Natl Acad. Sci. USA* **105,** 5856–5861 (2008).
5. Lindvall, O. & Kokaia, Z. Stem cells in human neurodegenerative disorders–time for clinical translation? *J. Clin. Invest.* **120,** 29–40 (2010).
6. Elkabetz, Y. *et al.* Human ES cell-derived neural rosettes reveal a functionally distinct early neural stem cell stage. *Genes Dev.* **22,** 152–165 (2008).
7. Roy, N. S. *et al.* Functional engraftment of human ES cell-derived dopaminergic neurons enriched by coculture with telomerase-immortalized midbrain astrocytes. *Nature Med.* **12,** 1259–1268 (2006).
8. Kittappa, R., Chang, W. W., Awatramani, R. B. & McKay, R. D. The *foxa2* gene controls the birth and spontaneous degeneration of dopamine neurons in old age. *PLoS Biol.* **5,** e325 (2007).
9. Ferri, A. L. *et al. Foxa1* and *Foxa2* regulate multiple phases of midbrain dopaminergic neuron development in a dosage-dependent manner. *Development* **134,** 2761–2769 (2007).
10. Roelink, H. *et al.* Floor plate and motor neuron induction by *vhh-1*, a vertebrate homolog of hedgehog expressed by the notochord. *Cell* **76,** 761–775 (1994).
11. Liem, K. F., Tremml, G., Roelink, H. & Jessell, T. M. Dorsal differentiation of neural plate cells induced by BMP-mediated signals from epidermal ectoderm. *Cell* **82,** 969–979 (1995).
12. Fasano, C. A., Chambers, S. M., Lee, G., Tomishima, M. J. & Studer, L. Efficient derivation of functional floor plate tissue from human embryonic stem cells. *Cell Stem Cell* **6,** 336–347 (2010).
13. Chambers, S. M. *et al.* Highly efficient neural conversion of human ES and iPS cells by dual inhibition of SMAD signaling. *Nature Biotechnol.* **27,** 275–280 (2009).
14. Muroyama, Y., Fujihara, M., Ikeya, M., Kondoh, H. & Takada, S. Wnt signaling plays an essential role in neuronal specification of the dorsal spinal cord. *Genes Dev.* **16,** 548–553 (2002).
15. Joksimovic, M. *et al.* Wnt antagonism of Shh facilitates midbrain floor plate neurogenesis. *Nature Neurosci.* **12,** 125–131 (2009).
16. Lyashenko, N. *et al.* Differential requirement for the dual functions of beta-catenin in embryonic stem cell self-renewal and germ layer formation. *Nature Cell Biol.* **13,** 753–761 (2011).
17. VanDunk, C., Hunter, L. A. & Gray, P. A. Development, maturation, and necessity of transcription factors in the mouse suprachiasmatic nucleus. *J. Neurosci.* **31,** 6457–6467 (2011).
18. Huang, W., Sherman, B. T. & Lempicki, R. A. Systematic and integrative analysis of large gene lists using DAVID bioinformatics resources. *Nature Protocols* **4,** 44–57 (2009).
19. Costa, R. H., Grayson, D. R. & Darnell, J. E., Jr. Multiple hepatocyte-enriched nuclear factors function in the regulation of transthyretin and alpha 1-antitrypsin genes. *Mol. Cell. Biol.* **9,** 1415–1425 (1989).
20. Soldner, F. *et al.* Parkinson's disease patient-derived induced pluripotent stem cells free of viral reprogramming factors. *Cell* **136,** 964–977 (2009).
21. Guzman, J. N., Sanchez-Padilla, J., Chan, C. S. & Surmeier, D. J. Robust pacemaking in substantia nigra dopaminergic neurons. *J. Neurosci.* **29,** 11011–11019 (2009).
22. Nedergaard, S., Flatman, J. A. & Engberg, I. Nifedipine- and omega-conotoxin-sensitive Ca^{2+} conductances in guinea-pig substantia nigra pars compacta neurones. *J. Physiol. (Lond.)* **466,** 727–747 (1993).
23. Ferrari, D., Sanchez-Pernaute, R., Lee, H., Studer, L. & Isacson, O. Transplanted dopamine neurons derived from primate ES cells preferentially innervate DARPP-32 striatal progenitors within the graft. *Eur. J. Neurosci.* **24,** 1885–1896 (2006).
24. Olanow, C. W., Kordower, J. H. & Freeman, T. B. Fetal nigral transplantation as a therapy for Parkinson's disease. *Trends Neurosci.* **19,** 102–109 (1996).
25. Zetterström, R. H. *et al.* Dopamine neuron agenesis in Nurr1-deficient mice. *Science* **276,** 248–250 (1997).
26. Quintana, E. *et al.* Efficient tumour formation by single human melanoma cells. *Nature* **456,** 593–598 (2008).
27. Kim, H. *et al.* miR-371-3 expression predicts neural differentiation propensity in human pluripotent stem cells. *Cell Stem Cell* **8,** 695–706 (2011).
28. Hargus, G. *et al.* Differentiated Parkinson patient-derived induced pluripotent stem cells grow in the adult rodent brain and reduce motor asymmetry in Parkinsonian rats. *Proc. Natl Acad. Sci. USA* **107,** 15921–15926 (2010).
29. Aubry, L. *et al.* Striatal progenitors derived from human ES cells mature into DARPP32 neurons *in vitro* and in quinolinic acid-lesioned rats. *Proc. Natl Acad. Sci. USA* **105,** 16707–16712 (2008).

Supplementary Information is linked to the online version of the paper at www.nature.com/nature.

Acknowledgements We thank K. Manova, M. Tomishima and A. Viale for excellent technical support, and R. McKay for the anti-nestin antibody. The work was supported by NIH/NINDS grant NS052671, the European Commission project NeuroStemcell, the Starr foundation and NYSTEM contract C024414 to L.S.; by NYSTEM contract C024413, the Michael T. McCarthy Foundation and the Elkus Family Foundation to V.T.; by the Consolidated Anti-Aging Foundation to J.H.K.; by NIH/NINDS grant P50 NS047085, and support from Falk Medical Research Trust to D.J.S.; J.-W.S. was supported by NYSCF (Druckenmiller fellowship) and S.K. by a Starr stem cell scholar fellowship.

Author Contributions S.K. and J.-W.S.: conception and study design, maintenance and directed differentiation of PSCs, cellular/molecular assays, histological analyses, mouse behavioural assays, data interpretation and writing of manuscript. J.P., G.A., C.A. and A.B.: rat transplantation, histological analyses and behavioural assays. Y.M.G.: mouse transplantation and histological analyses. D.R.W. and J.H.K.: monkey transplantation, histological analysis and data interpretation. L.Y. and M.F.B.: HPLC analysis and data interpretation. L.C.-R., Z.X and D.J.S.: electrophysiological analyses and data interpretation. V.T.: study design, data analysis and writing of manuscript. L.S.: conception and study design, data analysis and interpretation, and writing of manuscript.

Author Information The raw gene expression data generated in this study have been deposited in the Gene Expression Omnibus database under accession number GSE32658. Reprints and permissions information is available at www.nature.com/reprints. The authors declare no competing financial interests. Readers are welcome to comment on the online version of this article at www.nature.com/nature. Correspondence and requests for materials should be addressed to L.S. (studerl@mskcc.org).

METHODS

Culture of undifferentiated ES cells. ES cell lines H9 (WA-09, XX, passages 35–45), H1 (WA-01, XY, passages 30–40) and iPS cell lines 2C6 (XY, passages 20–30, ref. 27) and SeV6 (XY, passages 20–30; derived from MRC-5 using non-integrating 4 factor Sendai vector system[30]) were maintained on mouse embryonic fibroblasts (MEF, Global Stem) in 20% knockout serum replacement (KSR, Invitrogen)-containing ES cell medium as described previously[27].

Neural induction. For FP-based midbrain DA neuron induction, a modified version of the dual-SMAD inhibition[13] and FP induction[12] protocol was used based on timed exposure to LDN193189 (100 nM, Stemgent), SB431542 (10 μM, Tocris), SHH C25II (100 ng ml^{-1}, R&D), Purmorphamine (2 μM, Stemgent), FGF8 (100 ng ml^{-1}, R&D) and CHIR99021 (CHIR; 3 μM, Stemgent). Note: for the FP induction protocol we refer to 'SHH' treatment as exposure of cells to a combination of SHH C25II 100 ng ml^{-1} + purmorphamine (2 μM). Cells were plated (35×10^3–40×10^3 cells per cm^2) and grown for 11 days on matrigel (BD) in knockout serum replacement medium (KSR) containing DMEM, 15% knockout serum replacement, 2 mM L-glutamine and 10 μM β-mercaptoethanol. KSR medium was gradually shifted to N2 medium starting on day 5 of differentiation as described previously[13]. On day 11, media was changed to Neurobasal/B27/L-Glut containing medium (NB/B27; Invitrogen) supplemented with CHIR (until day 13) and with BDNF (brain-derived neurotrophic factor, 20n ml^{-1}; R&D), ascorbic acid (0.2 mM, Sigma), GDNF (glial cell line-derived neurotrophic factor, 20 ng ml^{-1}; R&D), TGFβ3 (transforming growth factor type β3, 1 ng ml^{-1}; R&D), dibutyryl cAMP (0.5 mM; Sigma), and DAPT (10 μM; Tocris,) for 9 days. On day 20, cells were dissociated using Accutase (Innovative Cell Technology) and replated under high cell density conditions (300×10^3–400×10^3 cells per cm^2) on dishes pre-coated with polyornithine (PO; 15 μg ml^{-1})/laminin (1 μg ml^{-1})/fibronectin (2 μg ml^{-1}) in differentiation medium (NB/B27 + BDNF, ascorbic acid, GDNF, dbcAMP, TGFβ3 and DAPT) until the desired maturation stage for a given experiment.

For rosette-based DA neuron induction we followed our previously described protocols[2] but used dual-SMAD inhibition to accelerate the initial neural induction step. In brief, ES cells were induced towards neural fate by co-culture with irradiated MS5 cells in KSR supplemented with SB431542 and Noggin (250 ng ml^{-1}; R&D), from day 2–8 and SHH + FGF8 from day 6–11 of differentiation. After 11 days in KSR, neural rosettes were manually isolated and cultured (P1 stage) in N2 medium supplemented with SHH, FGF8, BDNF and ascorbic acid as described previously[2]. After 5–7 days in P1 stage, rosettes were again harvested mechanically and triturated following incubation in Ca^2/Mg^2-free Hanks' balanced salt solution (HBSS) for 1 h and replated on PO/laminin/fibronectin-coated plates. Patterning with SHH/FGF8 was continued for 7 days at P2 stage followed by final differentiation in the presence of BDNF, ascorbic acid, GDNF, TGFb3 and dbcAMP as described above until the desired maturation stage for a given experiment (typically 5–7 days for transplantation studies or 32 days for *in vitro* functional studies).

Gene expression analyses. Total RNA was extracted during differentiation at days 0, 1, 3, 5, 7, 9, 11, 13 and 25 from each condition of control LSB, LSB/SHH/FGF8 and LSB/SHH/FGF8/CHIR using an RNeasy kit (Qiagen). For microarray analysis, total RNA was processed by the MSKCC Genomic core facility and hybridized on Illumina Human ref-12 bead arrays according to the specifications of the manufacturer. Comparisons were performed among each days and conditions using the LIMMA package from Bioconductor (http://www.bioconductor.org). Genes found to have an adjusted *P*-value <0.05 and a fold change greater than two were considered significant. Some of the descriptive microarray data analyses and presentation was performed using a commercially available software package (Partek Genomics Suite (version 6.10.0915)). For qRT–PCR analyses, total RNA at day 25 of each condition was reverse transcribed (Quantitech, Qiagen) and amplified material was detected using commercially available TaqMan gene expression assays (Applied Biosystems) with the data normalized to HPRT. Each data point represents nine technical replicates from three independent biological samples. Raw data of all the microarray studies are available at GEO http://www.ncbi.nlm.nih.gov/geo/ accession number GSE32658.

Animal surgery. All rodent and monkey procedures were performed following NIH guidelines, and were approved by the local Institutional Animal Care and Use Committee (IACUC), the Institutional Biosafety Committee (IBC) as well as the Embryonic Stem Cell Research Committee (ESCRO).

Mice: *NOD-SCID IL2Rgc* null mice (20–35 g; Jackson Laboratory) were anaesthetized with ketamine (90 mg kg^{-1}; Akorn) and xylazine (4 mg kg^{-1}). 6-hydroxydopamine (10 μg 6-OHDA, Sigma-Aldrich) was injected stereotactically into the striatum at the following coordinates (in millimetres): AP, 0.5 (from bregma); ML, −2.0; DV, −3.0 (from dura). Mice with successful lesions (an average of >6 rotations per minute) were selected for transplantation. A total of 1.5×10^5 cells were injected in a volume of 1.5 μl into the striatum at the following coordinates (in mm): AP, 0.5; ML, −1.8; DV, 3.2. The mice were killed 18 weeks after transplantation.

Rats: adult female Sprague Dawley (Taconic) rats (180–230 g) were anaesthetized with Ketamine (90 mg kg^{-1}) and xylazine (4 mg kg^{-1}) during surgical procedures. Unilateral, medial forebrain bundle lesions of the nigro-striatal pathway were established by stereotaxic injection of 6-OHDA (3.6 mg ml^{-1} in 0.2% ascorbic acid and 0.9% saline, Sigma) at two sites[31]. Rats were selected for transplantation if amphetamine-induced rotation exceeded 6 rotations per min by 6–8 weeks post injection. 2.5×10^5 cells were transplanted into the striatum of each animal (Coordinates: AP 1.0 mm, ML −2.5 mm and V −4.7 mm; toothbar set at −2.5). Control rats received PBS instead. The surgical procedures were described previously[31]. Daily intraperitoneal injections of cyclosporine 15 mg kg^{-1} (Bedford Labs) were started 24 h before cell grafting and continued until death, 20 weeks following cell grafting.

Primates: two adult (17–18 year old; 10–12 kg; female) rhesus monkeys were rendered hemiparkinsonian via carotid MPTP administration followed by weekly intravenous MPTP administration to create a bilateral parkinsonian syndrome[32]. Both animals displayed parkinsonian symptoms consistent with a moderately-severe lesion. On the day of transplantation surgery, animals were tranquilized with ketamine (3.0 mg kg^{-1}, intramuscular) and dexdomitor (0.02-0.04 mg kg^{-1} intramuscular), intubated to maintain a stable airway and anaesthetized with isoflurane. They were then placed into a stereotaxic frame for surgery. Both rhesus monkeys underwent a single surgery with three intracranial injections of human FP-derived DA cultures based on stereotaxic coordinates[33]. Bilateral injections of cells (10 μl/injection; 125,000 cells per μl) were performed at three sites (one posterior caudate, two pre-commissural putamen and overlying white matter) for a total volume of 30 μl per hemisphere. An infusion pump attached to a stereotaxic micromanipulator was used to deliver the cells at a rate of 1 μl min^{-1} though a 50-μl Hamilton syringe with 28 G needle. After the injections were completed, the needle was left in place for an additional 2–5 min to allow the infusate to diffuse off the needle tip before slowly retracting the syringe. Immediately following surgery, the animals received analgesics (buprenex, 0.01 mg kg^{-1} intramuscular, BID for 72 h post surgery; meloxicam, 0.1 mg kg^{-1} subcutaneous, SID for 72 h post surgery) as well as an antibiotic (cephazolin, 25 mg kg^{-1} intramuscular, BID) until 72 h post-surgery. The animals received cyclosporine A (Neoral, Sandimmune) orally (30 mg kg^{-1} tapered to 15 mg kg^{-1}) once daily beginning 48 h before surgery until death, one month following transplantation.

Behavioural assays. Amphetamine-induced rotations (mice and rats) and the stepping test (rat) were carried out before transplantation and 4, 8, 12 and 18 weeks after transplantation. Rotation behaviour in mice was recorded 10 min after intraperitoneal injection of d-amphetamine (10 mg kg^{-1}, Sigma) and recorded for 30 min. Rotation behaviour in rats was recorded 40 min after intraperitoneal injection of d-amphetamine (5 mg kg^{-1}) and automatically assessed by the TSE VideoMot2 system (Germany). The data were presented as the average number of rotations per minute. The stepping test was modified from[34,35]. In brief, each rat was placed on a flat surface, its hind legs were lifted by gently holding up the tail to allow only the forepaws to touch the table. The experimenter pulled the rat backwards 1 m at a steady pace. Adjusting step numbers from both contralateral and ipsilateral forepaws were counted. Data was presented as the percentage of contralateral/(contralateral + ipsilateral) adjusting steps. The cylinder test was performed by placing each animal in a glass cylinder and counting the number of ipsilateral versus contralateral paw touches (out of 20 touches) to the wall of the cylinder as described previously[3].

Tissue processing. Mice and rats received overdoses of pentobarbital intraperitoneally (50 mg kg^{-1}) to induce deep anaesthesia and were perfused in 4% paraformaldehyde (PFA). Brains were extracted, post-fixed in 4% PFA then soaked in 30% sucrose solutions for 2–5 days. They were sectioned on a cryostat after embedding in O.C.T. (Sakura-Finetek).

Primates were killed under deep anaesthesia with ketamine (10 mg kg^{-1}, intramuscular) and pentobarbital (25 mg kg^{-1}, intravenous) via cardiac perfusion with heparinized 0.9% saline followed by fresh cold 4% PFA fixative (pH 7.4). Immediately following primary fixation, brains were removed from the skull and post-fixed in 4% PFA, free-floating, for 24–36 h. They were then rinsed and re-suspended in 10% sucrose on a slow shaker at 4 °C, and allowed to 'sink'. The process was then repeated in 20% sucrose followed by 30% sucrose. Whole brains were cut coronally into 40 μm serial sections on a frozen sledge microtome and stored free-floating in cryopreservative medium at −20 °C.

Immunohistochemistry. Cells were fixed in 4% PFA and blocked with 1% BSA with 0.3% Triton. Brain tissue sections were washed in cold PBS and processed similarly. Primary antibodies were diluted in 1–5% BSA or Normal Goat Serum and incubated according to manufacturer recommendations. A comprehensive list of antibodies and sources is provided as Supplementary Table 6. Appropriate

Alexa488, Alexa555 or Alexa647-conjugated secondary antibodies (Molecular Probes) were used with 4′,6-diamidino-2-phenylindole (DAPI) nuclear counterstain (Thermo Fisher). For some analyses biotinylated secondary antibodies were used followed by visualization via DAB chromogen.

HPLC analysis. Reversed-phase HPLC with electrochemical detection for measuring levels of DA, HVA and DOPAC was performed as described previously[7,36]. Culture samples were collected in perchloric acid at day 65 of differentiation. For some experiments DA was measured directly in the medium using the same detection system but following aluminium extraction of DA and its metabolites using a commercially available kit as described previously[36].

Electrophysiological recordings. Cultures were transferred to a recording chamber on an upright microscope equipped with a ×40 water-immersion objective (Eclipse E600FN; Nikon); cultures were perfused with saline containing in mM: 125 NaCl, 2.5 KCl, 25 $NaHCO_3$, 1.25 NaH_2PO_4, 2 CaCl, 1 $MgCl_2$ and 25 glucose (34 °C; saturated with 95% 0_2/5% CO_2; pH 7.4; 298 mOsm l^{-1}). The saline flow rate was 2–3 ml min^{-1} running through an in-line heater (SH-27B with TC-324B controller; Warner Instruments). Neurons were visualized by video microscopy with a cooled-CCD digital camera (CoolSNAP ES^2, Photometrics, Roper Scientific). Cells selected for electrophysiological recordings had neuron-like shapes with fine branching neurites. Somatic whole-cell patch-clamp recordings in current clamp configuration were performed with a MultiClamp 700B amplifier (Molecular Devices). Signals were filtered at 1–4 kHz and digitized at 5–20 kHz with a Digidata 1440A (Molecular Devices). Recording patch electrodes were fabricated from filamented borosilicate glass (Sutter Instruments) pulled on a Flaming-Brown puller (P-97, Sutter Instruments) and had resistances of 4–6 MΩ in the bath. Electrodes were filled with internal solution containing in mM: 135 K-$MeSO_4$, 5 KCl, 5 HEPES, 0.25 EGTA, 10 phosphocreatine-di(tris), 2 ATP-Mg and 0.5 GTP-Na (pH 7.3, osmolarity adjusted to 290-300 mOsm l^{-1}). The amplifier bridge circuit was adjusted to compensate for electrode resistance and monitored. Electrode capacitance was also compensated. If series resistance increased >20% during the recording, the data were discarded.

Cell counts and stereological analyses. The percentages of marker positive cells at the FP (day 11), midbrain DA neuron precursor (day 25) and mature DA neuron stages (day 50 or later) were determined in samples derived from at least three independent experiments each. Images for quantification were selected in a uniform random manner and each image was scored first for the number of DAPI-positive nuclei, followed by counting the number of cells expressing the marker of interest. All data are presented as mean ± s.e.m. Quantification of human cells (identified with anti-human nuclear antigen) and TH+ neurons within grafts was performed on every tenth section where a graft was identifiable. Cell counts and graft volume were determined using the optical fractionator probe and the Cavalieri estimator using the Stereo Investigator software (MBF bioscience, Vermont) as described previously[37]. Data are presented as estimated total cell number and total graft volume ±s.e.m. Statistical analysis was performed using the Student *t*-test (comparing two groups) or ANOVA with Dunnett test (comparing multiple groups against control).

30. Ban, H. *et al.* Efficient generation of transgene-free human induced pluripotent stem cells (iPSCs) by temperature-sensitive Sendai virus vectors. *Proc. Natl. Acad. Sci. USA* **108,** 14234–14239 (2011).
31. Studer, L., Tabar, V. & McKay, R. D. Transplantation of expanded mesencephalic precursors leads to recovery in parkinsonian rats. *Nature Neurosci.* **1,** 290–295 (1998).
32. Kordower, J. H. *et al.* Neurodegeneration prevented by lentiviral vector delivery of GDNF in primate models of Parkinson's disease. *Science* **290,** 767–773 (2000).
33. Paxinos, G., Huang, X.-F. & Toga, A. W. *The Rhesus Monkey Brain in Stereotaxic Coordinates* (Academic Press, 2000).
34. Blume, S. R., Cass, D. K. & Tseng, K. Y. Stepping test in mice: a reliable approach in determining forelimb akinesia in MPTP-induced Parkinsonism. *Exp. Neurol.* **219,** 208–211 (2009).
35. Crawley, J. N. *What's Wrong With My Mouse: Behavioral Phenotyping of Transgenic and Knockout Mice* (Wiley, 2000).
36. Studer, L. *et al.* Noninvasive dopamine determination by reversed phase HPLC in the medium of free-floating roller tube cultures of rat fetal ventral mesencephalon: A tool to assess dopaminergic tissue prior to grafting. *Brain Res. Bull.* **41,** 143–150 (1996).
37. Tabar, V. *et al.* Migration and differentiation of neural precursors derived from human embryonic stem cells in the rat brain. *Nature Biotechnol.* **23,** 601–606 (2005).